Enhanced amplified spontaneous emission using layer-by-layer assembled cowpea mosaic virus

Na Li, Zhaoqi Deng, Yuan Lin, Xiaojie Zhang, Yanhou Geng, Dongge Ma,[a] and Zhaohui Su[b]

State Key Laboratory of Polymer Physics and Chemistry, Changchun Institute of Applied Chemistry and Graduate School of Chinese Academy of Sciences, Chinese Academy of Sciences, Changchun 130022, People's Republic of China

(Received 25 June 2008; accepted 17 November 2008; published online 6 January 2009)

Layer-by-layer assembly technique was used to construct ultrathin film of cowpea mosaic virus (CPMV) by electrostatic interactions, and the film was employed as a precursor on which an OF8T2 film was deposited by spin coating. Amplified spontaneous emission (ASE) was observed and improved for the OF8T2 film. Compared with OF8T2 film on quartz, the introduction of CPMV nanoparticles reduced the threshold and loss, and remarkably increased the net gain. The threshold, loss, and gain reached 0.05 mJ/pulse, 6.9 cm^{-1}, and 82 cm^{-1}, respectively. CPMV nanoparticles may enormously scatter light, resulting in a positive feedback, thus the ASE is easily obtained and improved. © *2009 American Institute of Physics*. [DOI: 10.1063/1.3056137]

I. INTRODUCTION

Since the demonstration of the first laser made with ruby in 1960, a great deal of research has been focused on the study of amplified spontaneous emission (ASE) and lasing action from various materials.[1,2] The properties of materials as gain media play an important role in the performance of lasers, and many efforts have been devoted to the synthesis of new materials as the gain mediums to obtain high performance ASE and lasing.[3,4] Furthermore, on the basis of new materials, many feedback structures and methods, such as distributed feedback resonator,[5] encapsulating coumarin 151 in mesoporous SBA-15,[6] codoping of two dyes,[7] and introduction of gold nanoparticles,[8] have also been developed to further improve the ASE and lasing performance.

Construction of ultrathin films via electrostatic layer-by-layer (LbL) assembly technique has been developed rapidly in the past decade.[9,10] This method is suitable for the fabrication of functional ultrathin films with highly tunable surface on a variety of substrates. Cowpea mosaic virus (CPMV), a plant virus with a monodisperse diameter of ~30 nm, is composed of 60 copies of two protein subunits in an icosahedral symmetry and has been studied extensively as a model system.[11] Its regular nanostructure should also be proper as scattering to supply a positive feedback on the realization of ASE or lasing based on organic materials. However, this structure has not been explored in this aspect.

In this work, LbL assembly technique was used to construct ultrathin film of CPMV by electrostatic interactions, and we used this kind of nanostructure as scattering feedback to study the ASE of a monodisperse oligomer, oligo(9,9′-dioctylfluorene-*co*-bithiophene) (OF8T2). An ASE was observed and the properties of threshold, gain, and loss were improved.

[a]Tel.: +86-431-85262357. FAX: +86-431-85262873. Electronic mail: mdg1014@ciac.jl.cn.

[b]Author to whom correspondence should be addressed. Tel.: +86-431-85262854. FAX: +86-431-85262126. Electronic mail: zhsu@ciac.jl.cn.

II. EXPERIMENTAL PROCEDURE

Poly(diallyldimethylammonium chloride) (PDDA) aqueous solution (molecular weight 100 000–200 000) and poly(styrene sulfonate) (PSS) (M_W=70 000) were purchased from Aldrich Co. The wild-type CPMV was kindly provided by Professor Wang. Monodisperse OF8T2 (M_W=1495.44, polydispersity index=1.03) was synthesized as previously reported.[4]

Quartz crystal microbalance (QCM) was employed to investigate the LbL assembly process. The frequency was monitored by a Protek frequency counter (model C3100). AT-cut quartz crystals with Ag electrodes deposited were manufactured by Beijing Ziweixing Microelectronic Co., Ltd. A quartz crystal was immersed in a PDDA aqueous solution (1.0 mg/ml) for 20 min, removed and washed thoroughly with pure water, and dried with a stream of N_2 gas. The positively charged surface was then immersed in a PSS aqueous solution (1.0 mg/ml) for 20 min, removed and rinsed with water, and dried with N_2. The cycle was repeated three times and then the crystal was dipped in the PDDA solution to deposit a PDDA outmost layer on the three PDDA/PSS bilayers assembled on the quartz substrate. The electrode with a $(PDDA/PSS)_3/PDDA$ multilayer coating was then alternately immersed in a CPMV solution (0.1 mg/ml, *p*H=4) and a PDDA solution, each for 20 min with water rinse and N_2 blowing in between, and the deposition cycle was repeated until a desired number of layers was obtained. The approach is illustrated in Fig. 1(a).

The ASE properties of the films were investigated using the experimental setup as described elsewhere.[6,7] The pump source was a frequency-tripped neodymium doped yttrium aluminum garnet laser (Spectra-Physics) emitting 10 ns pulses at λ_p=355 nm with a 10 Hz repetition rate. The output pulse energy of the pump laser was controlled by neutral-density filters. An adjustable slit and a cylindrical lens were used before the beam splitter in order to shape the beam into a narrow stripe with a continuously varied length on the sample film. The films were pumped at normal incidence

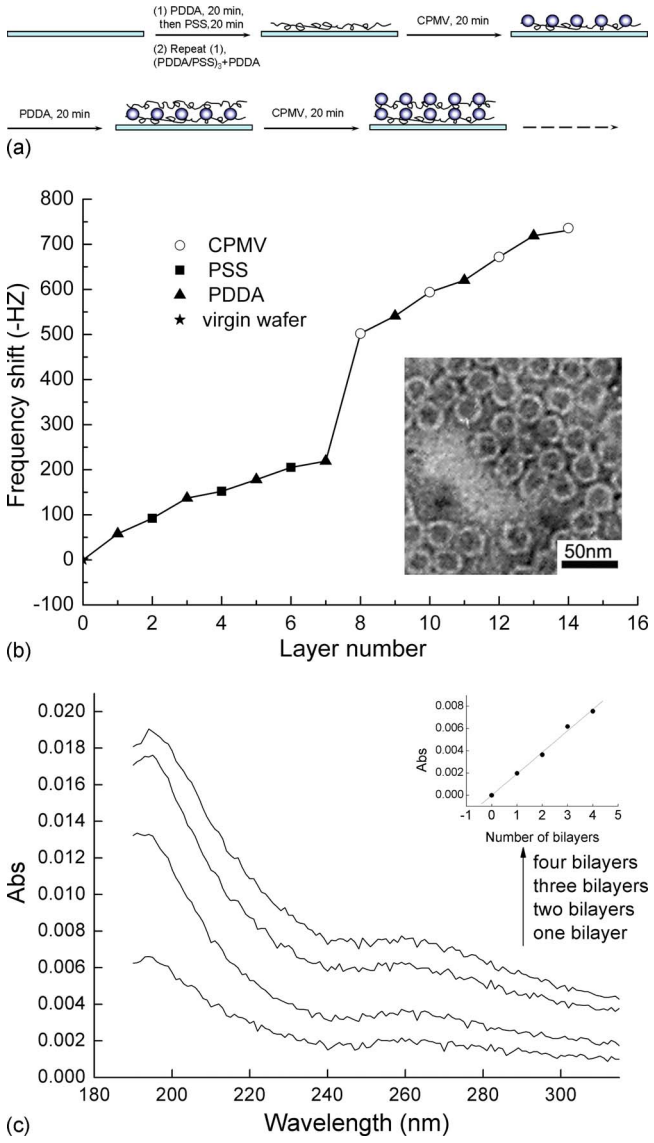

FIG. 1. (Color online) (a) Schematic illustration of the stepwise growth of the multilayer film. (b) QCM frequency shifts for alternating adsorptions of PDDA (▲) and PSS (■) for three times, then PDDA (▲) and CPMV (○) on virgin quartz electrode (★). The inset shows the TEM image of the CPMV assembled. (c) UV-visible absorption spectra of PDDA/CPMV multilayer films with different numbers of bilayers. The inset shows the UV absorbance at 260 nm as a function of number of bilayers.

with the long axis of the pump beam perpendicular to the edge of the sample. The output signals were detected by a fiber-coupled charge coupled device spectrometer (JY Spex CCD3000). The pumped energies from the laser were measured using a calibrated laser power and energy meter (Gentec).

III. RESULTS AND DISCUSSION

CPMV has an isoelectric point (IEP) of 5.5, and it is stable in a solution indefinitely at room temperature in the *p*H region of 3.5–9.0. At *p*H=4.0, below its IEP, although the net charge the CPMV carries is positive, there are still negative charges exposed on the exterior of the surface of the CPMV,[12] and therefore the CPMV nanoparticles can adsorb to the positively charged PDDA surface via electrostatic interaction. Under this condition, the repulsion between the particles and the surface restrains the nanoparticles from aggregation.

The transmission electron microscopy image of the CPMVs is shown in the inset of Fig. 1(b), which shows that the diameter of the CPMW is approximately 30 nm, and the thickness of the capsule is about 4 nm. QCM frequency shift was monitored in each adsorption step, and the data are presented in Fig. 1(b). The data show a stable tendency of growth with each layer deposition. The frequency shift for the first CPMV layer was about 283 Hz and by applying Sauerbrey equation,[13] this indicated a mass of 123 ng of CPMV adsorbed to each side of the QCM electrode, which corresponded to 83% surface coverage assuming spherical packing of the CPMV with a monolayer adsorption. The average frequency shift for each subsequent CPMV layer of CPMV was about 50 Hz, and after four PDDA/CPMV deposition cycles, CPMV nanoparticles covered the substrate completely. UV-visible spectra of the thin films were collected on a Shimadzu UV-2450 spectrophotometer to monitor the growth of the layers, and the spectra of PDDA/CPMV films with different numbers of assembly cycles are shown in Fig. 1(c). Since PDDA has only a slight absorbance in the far-UV region,[14] the spectrum of the CPMV/PDDA film mostly corresponds to that of CPMV. The absorbance at about 260 nm corresponds to the aromatic amino acid residues in the CPMV, which is plotted against the number of bilayers assembled, and a linear growth pattern is observed in the inset of Fig. 1(c). This indicates that the LbL assembly of PDDA and CPMV was steady and uniform.

An OF8T2 film was produced by spin coating a chloroform solution of OF8T2 (15 mg/ml) on a $(PDDA/PSS)_3/(PDDA/CPMV)_4$ multilayer film deposited on quartz by LbL assembly method described above. In addition, a CPMV film was first produced by casting a CPMV aqueous solution (0.01 mg/ml, *p*H=4) on a quartz substrate, on top of which an OF8T2 film then was spin coated from the chloroform solution (15 mg/ml). As a control sample, an OF8T2 film on a quartz substrate was prepared by spin coating.

The OF8T2 structure is shown in Fig. 2(a). All OF8T2 films fabricated by spin coating exhibited ASE. Below the threshold pumping energy, the emission spectrum exhibited a broad and weak peak of spontaneous emission with a full width at half maximum (FWHM) of about 22 nm. As the pumping energy increased to above the threshold, ASE emission became dominant. The output intensity sharply increased and FWHM of the emission spectrum was substantially reduced to about 4 nm [Fig. 2(b)]. This collapse of the FWHM in emission spectrum is one of the signatures of the presence of ASE.

To particularly demonstrate the effect of CPMV on ASE, the threshold, gain, and loss of an OF8T2 film on quartz were compared with that of OF8T2 films on a CPMV layer cast and on a CPMV assembly produced by LbL technique, respectively. The output emission intensity integrated over all wavelengths as a function of the pumped energy is shown in Fig. 3(a). When the pump energy is below the threshold value, the emission intensity is low and increases in propor-

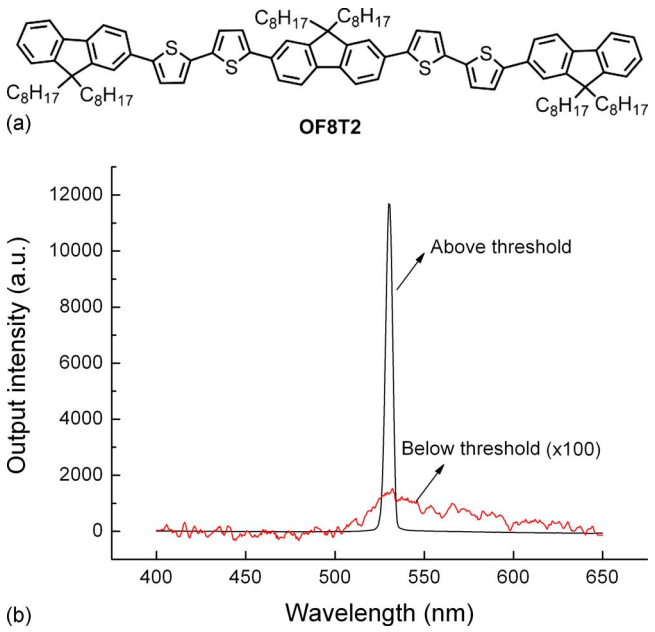

FIG. 2. (Color online) (a) Structure of the conjugated oligomer OF8T2. (b) Emission spectra of OF8T2 films pumped by optically pulsed laser at above and below lasing threshold (the latter is multiplied by a factor of 100).

tion to the pump intensity slowly. As the pump energy is above the threshold, the emission intensity increases sharply. Therefore the threshold pump energy for ASE can be easily discerned at 0.055, 0.087, and 0.050 mJ pulse^{-1} for OF8T2 film on quartz, on cast CPMV and on CPMV assembled, respectively.

The net gain of the film was measured by the variable stripe length method reported in literature.[3,6] The emission intensity from the film edge was recorded and plotted against the excitation length. Figure 3(b) displays the dependence of the emission intensity at λ_{ASE} on the excitation length at 0.11 mJ pulse^{-1}. The output intensity I of the ASE is given by the relationship

$$I = \frac{A(\lambda) Ip}{g(\lambda)} (\exp^{g(\lambda) l} - 1), \quad (1)$$

where $A_{(\lambda)}$ is a constant related to the emission cross section, I_p the pumped energy intensity, l the length of the pumped stripe, and $g_{(\lambda)}$ the net gain coefficient. The net gain $g_{(\lambda)}$ can be obtained by fitting the experimental data to Eq. (1) as the solid curves shown in Fig. 3(b). The net gain was 14 cm^{-1} for OF8T2 film on quartz, whereas the net gains reached 53 and 82 cm^{-1} for OF8T2 film on cast CPMV and CPMV multilayer assembly, respectively, which were much higher than that for the emissive film on quartz. Obviously, the introduction of the CPMV film greatly enhanced the ASE gain

For evaluating the loss coefficient in the waveguides, the pumped length was kept constant (l=0.3 cm), and the strip was gradually moved away from the film edge. Since the emission from the end of the pump stripe remains constant, the detected signal from the edge of the sample decreases as waveguide loss within the unpumped region, and this follows the Beer–Lambert law

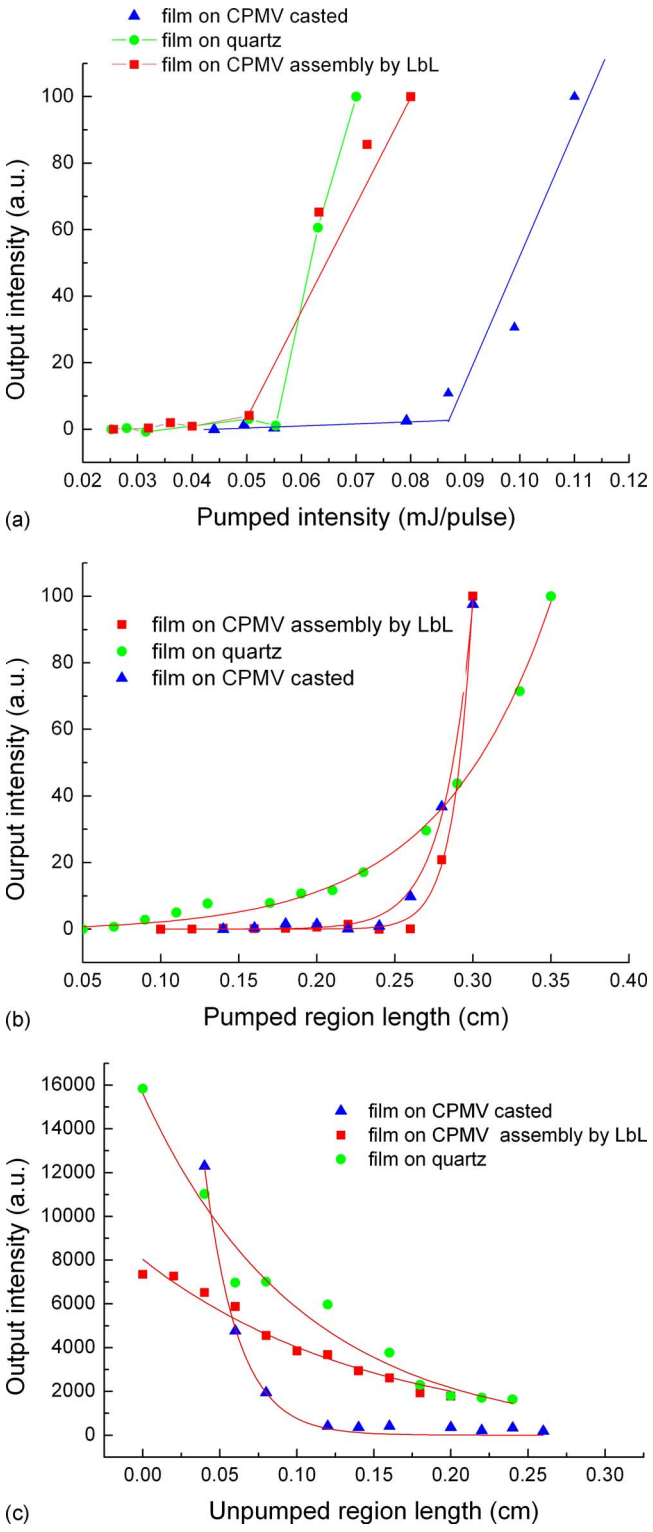

FIG. 3. (Color online) (a) Output emission intensity integrated over all wavelengths as a function of pumped intensity. (b) Dependence of the emission intensity at peak wavelength on the excitation length at indicated intensities. (c) Intensity of light emitted at peak wavelength from edge of a waveguide as a function of the distance between the pump stripe and the edge of the film. [Note: curves in (a) and (b) are normalized to fit in the same plot. The maximum intensity data point in each curve is arbitrarily assigned a value of 100.]

$$I = I_0 \exp^{(-\alpha L)}, \quad (2)$$

where α is the waveguide loss coefficient, L is the length of the unpumped region from the end of the pump region to the

TABLE I. Threshold, gain, and loss of OF8T2 films.

System	λ_{ASE} (nm)	I_{th} (mJ pulse^{-1})	Gain (cm^{-1})	Loss (cm^{-1})
Film on quartz	534	0.055	14	9.8
Film on cast CPMV	533	0.087	53	46
Film on CPMV LbL assembly	534	0.05	82	6.9

edge of the sample, I_0 is a fitting parameter proportional to the emission intensity at the excited region, and I is the intensity after propagation through an unpumped region finally into the detector. Figure 3(c) shows the detected emission intensity as a function of stripe distance from film edge. Experimental data were fitted to Eq. (2), and the loss coefficient can be estimated as the solid line shown in Fig. 3(c). A loss coefficient of 9.8 cm^{-1} was obtained for the film on quartz, which was higher than the loss coefficient (6.9) for the film on the CPMV LbL assembly. However, the OF8T2 on CPMV cast film exhibited a much higher loss coefficient of 46 cm^{-1}.

The ASE threshold, gain, and loss values for the three systems are summarized in Table I. It can be seen that the OF8T2 film on CPMV LbL assembly exhibits the best ASE performance, with low threshold, high gain, and small loss. This indicates that the nanoparticle structure formed by the LbL approach plays an important role in improving ASE performance.

We attribute the improvement in ASE performance to the difference in the surface morphology on the substrate. The surface morphology was observed by tapping mode atomic force microscopy (AFM) (SPA 300, Seiko). As shown in Fig. 4, the quartz is smooth and flat with the smallest roughness with a root mean square (rms) of 0.51 nm. The spheres in the CPMV cast layer absorb on the substrate sporadically, and the CPMV spheres with a diameter of about 30 nm aggregate, leading to the largest roughness with a rms of 32.1 nm. On the other hand, via the LbL assembly process, CPMV nanoparticles cover the substrate completely and pack densely and evenly with very little aggregation, resulting in a small roughness with a rms of 4.2 nm. The CPMV nanoparticles may scatter light enormously, and multiple scattering keeps the light circulating in the OF8T2 film long enough, leading to positive feedback homologous to random lasing process in disordered media, and the gains exceed the losses, so ASE is easily obtained, and the ASE performance is improved. The OF8T2 film on cast CPMV exhibited a high loss coefficient of 46 cm^{-1} because the very rough surface induces great scattering losses within the unpumped region.

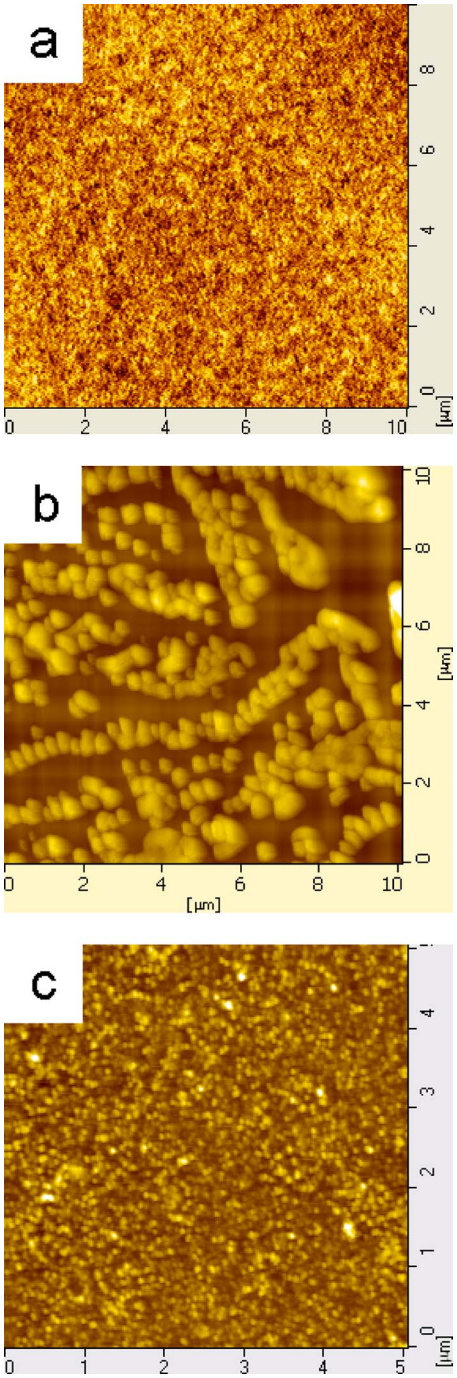

FIG. 4. (Color online) AFM images of (a) quartz surface, (b) CPMV nanoparticles cast on quartz, and (c) CPMV nanoparticles assembled via LbL process.

IV. CONCLUSION

In conclusion, we have investigated enhanced ASE performance of OF8T2 film by introducing viral capsids, CPMV, via LbL assembly. This CPMV-modified film showed the lowest threshold of 0.05 mJ pulse^{-1}, the highest net gain of 82 cm^{-1}, and the smallest loss coefficient of 6.9 cm^{-1}. The improvement of ASE performance has been attributed to positive feedback induced by CPMV nanoparticles as a result of multiple light scattering within the excited volume. The system may have potential for application as a feedback structure in organic lasers.

ACKNOWLEDGMENTS

This work was supported by the National Natural Science Foundation of China (Contract Nos. 20423003 and 20774097). Z.S. thanks the NSFC Fund for Creative Research Groups (Contract No. 50621302) for support.

[1]G. Heliotis, D. D. C. Bradley, G. A. Turnbull, and I. D. W. Samuel, Appl. Phys. Lett. **81**, 415 (2002).
[2]M. D. McGehee, M. A. Diaz-Garcia, F. Hide, R. Gupta, E. K. Miller, D. Moses, and A. J. Heeger, Appl. Phys. Lett. **72**, 1536 (1998).
[3]I. D. W. Samuel and G. A. Turnbull, Chem. Rev. (Washington, D.C.) **107**, 1272 (2007).
[4]X. J. Zhang, Y. Qu, L. J. Bu, H. K. Tian, J. P. Zhang, L. X. Wang, Y. H. Geng, and F. S. Wang, Chem. Eur. J. **13**, 6238 (2007).
[5]C. Karnutsch, C. Pflumm, G. Heliotis, J. C. Demello, D. D. C. Bradley, J. Wang, T. Weimann, V. Haug, C. Gartner, and U. Lemmer, Appl. Phys. Lett. **90**, 131104 (2007).
[6]D. K. Zhang, S. M. Zhang, D. G. Ma, Gulimina, and X. T. Li, Appl. Phys. Lett. **89**, 231112 (2006).
[7]D. K. Zhang and D. G. Ma, Appl. Opt. **46**, 2996 (2007).
[8]O. Popov, A. Zilbershtein, and D. Davidov, Polym. Adv. Technol. **18**, 751 (2007).
[9]A. A. Mamedov and N. A. Kotov, Langmuir **16**, 5530 (2000).
[10]Y. Lvov, K. Ariga, I. Ichinoe, and T. Kunitake, J. Am. Chem. Soc. **117**, 6117 (1995).
[11]G. P. Lomonossoff and J. E. Johnson, Prog. Biophys. Mol. Biol. **55**, 107 (1991).
[12]A. Chatterji, W. F. Ochoa, T. Ueno, T. W. Lin, and J. E. Johnson, Nano Lett. **5**, 597 (2005).
[13]G. Sauerbrey, Z. Phys. **155**, 206 (1959).
[14]T. Shutava, M. Prouty, D. Kommireddy, and Y. Lvov, Macromolecules **38**, 2850 (2005).